Title

Low-Molecular-Weight Protein Tyrosine Phosphatase Promotes Prostate Cancer Growth and Metastasis

Author

Nguyen, Tiffany Phuong

Publication Date

2021

Peer reviewed|Thesis/dissertation

UNIVERSITY OF CALIFORNIA SAN DIEGO

Low-Molecular-Weight Protein Tyrosine Phosphatase Promotes Prostate Cancer Growth and Metastasis

A Thesis submitted in satisfaction of the requirements

for the degree Master of Science

in

Biology

by

Tiffany Nguyen

Committee in charge:

Professor Stephanie Stanford, Chair
Professor Enfu Hui, Co-chair
Professor Aaron Coleman

2021

The Thesis of Tiffany Nguyen is approved, and it is acceptable in quality and form for publication on microfilm and electronically:

University of California San Diego

2021

DEDICATION

In recognition of my parents who have shown me an endless amount of love, support, care, and joy. Without you, I would not be where I am today, and I will never be able to express how much your love and support guides me.

In recognition of my family and friends for their unyielding support.

In recognition of Dr. Stephanie Stanford who took a chance on an inexperienced undergrad. Without your time, guidance, and support, I would not have grown this much as a researcher nor discovered my passion for research.

In recognition of everyone at the Bottini/Stanford lab for all the insight, input, and help in crafting my experiments.

TABLE OF CONTENTS

LIST OF ABBREVIATIONS

1x Pen/Strep: 100 U/mL penicillin & 100 µg/mL streptomycin

Ab: antibody

ACP1: Acid Phosphatase 1 gene

ANOVA: analysis of variance

ATF4: activating transcription factor 4

C4-2B: subline of LNCaP cells

Cas9: CRISPR associated protein 9

cDNA: complementary DNA

c-Myc: oncogene that is associated with cell cycle progression and apoptosis

Compd. 23: LMPTP inhibitor compound #23

Compd.: compound

CRISPR: clustered regularly interspaced short palindromic repeats

CST: Cell Signaling Technology

DI: deionized water

DMEM: Dulbecco's minimal essential medium

DMSO: dimethyl sulfoxide

EDTA: ethylenediamine tetra acetic acid

EIF2: eukaryotic initiation factor 2

EIF4: eukaryotic initiation factor 4

FACS: fluorescence-activated cell sorting

FBS: fetal bovine serum

Fe-NTA: ferric nitrilotriacetate

GAPDH: glyceraldehyde-3-phosphate dehydrogenase

GCN2: general control non-depressible 2

gDNA: genomic DNA

GFP: green fluorescence protein

GFP+: cells containing green fluorescence protein

gRNA: guide RNA

GSH: glutathione

GSSG: glutathione disulfide

HEPES: 4-(2-hydroxyethyl)-1-piperazineethanesulfonic acid

HRI: heme-regulated inhibitor

IACUC: Institutional Animal Care and Use Committee

IPA: Ingenuity Pathway Analysis

ISR: integrated stress response

IVIS: *in vivo* imaging system

KO: knockout

LC-MS/MS: liquid chromatography with tandem mass spectrometry

LMPTP: low-molecular-weight protein tyrosine phosphatase

LNCaP: human prostate cancer cell line derived from lymph node metastasis

Luc-Myc-CaP: luciferase-expressing Myc-CaP

MS: mass spectrometry

Myc-CaP: mouse prostate cancer cell line derived from a Hi-Myc mouse

NRF2: nuclear factor erythroid 2–related factor 2

PBS: phosphate buffered saline

PCA: principal component analysis

PCR: polymerase chain reaction

PERK: PKR-like endoplasmic reticulum kinase

PKR: protein kinase double-stranded RNA-dependent

POLR2A: RNA Polymerase II Subunit A

PRAD: prostate adenocarcinoma

PRL: phosphatases of regenerating liver

PTP: protein tyrosine phosphatase

p-value: statistical significance

qPCR: quantitative polymerase chain reaction

RLU: relative light units

ROS: reactive oxygen species

RPMI 1640 medium: Roswell Park Memorial Institute 1640 medium

RTK: receptor tyrosine kinase

SCID: severe combined immunodeficiency

SDS-PAGE: sodium dodecyl sulfate-polyacrylamide gel electrophoresis

SEM: standard error of the mean

SHP2: Src homology domain containing phosphatase 2

TBS-T: Tris-buffered saline with Tween 20

TCGA: The Cancer Genome Atlas

TMT: tandem mass tag

UHPLC-MS: ultrahigh performance liquid chromatography coupled to mass spectrometry

w/w: weight by weight

WB: western blot

WT: wild-type

LIST OF FIGURES

ACKNOWLEDGEMENTS

I would like to acknowledge Dr. Stephanie Stanford for her limitless support and guidance these past couple of years. She has been instrumental in both the development of this project and my personal growth as a researcher.

I would also like to acknowledge Joseph Chang for his hard work in getting this project started and complete trust in me for finishing it.

Lastly, I would like to acknowledge Dr. Enfu Hui and Dr. Aaron Coleman for being members of my thesis committee and incredibly supportive of my thesis project.

Figures 2 and 3 are coauthored by Joseph Chang and Tiffany Nguyen. Both authors contributed equally.

Figure 4 is coauthored by Joseph Chang, Michael Diaz, and Tiffany Nguyen. Tiffany Nguyen is the secondary author.

Figure 5 is coauthored by Joseph Chang and Tiffany Nguyen. Tiffany Nguyen is the primary author.

Figure 7 is coauthored by Dr. Arminja Kettenbach and Tiffany Nguyen. Both authors contributed equally.

Figure 8 is coauthored by Lavender Hackman, Dr. Stefano Tiziani, and Tiffany Nguyen. All authors contributed equally.

ABSTRACT OF THE THESIS

Low-Molecular-Weight Protein Tyrosine Phosphatase Promotes Prostate Cancer Growth and Metastasis

by

Tiffany Nguyen

Master of Science in Biology

University of California San Diego, 2021

Professor Stephanie Stanford, Chair

Professor Enfu Hui, Co-Chair

Currently, prostate adenocarcinoma (PRAD) is the second most common cancer in males, and the metastatic progression of prostate tumors to the bone accounts for a large majority of prostate cancer-related deaths. As such, identifying potential therapeutic targets to prevent prostate cancer progression proves to be vital. The low-molecular-weight protein tyrosine phosphatase (LMPTP) has been found to be highly expressed in metastatic hormone-naïve prostate cancer patients and is associated with lower survival rates. However, the molecular mechanism by which LMPTP promotes prostate cancer growth and metastatic development remains unclear. In this paper, we confirmed the oncogenic nature of LMPTP in prostate cancer growth *in vitro* and *in vivo* using both CRISPR-Cas9-mediated knockout (KO) of LMPTP and inhibition of LMPTP via an orally bio-available LMPTP inhibitor. Additionally, the use of a soft agar colony formation assay, Matrigel invasion chamber assay, and in vivo intraosseous metastasis model further implicated LMPTP in metastatic prostate cancer development. Through phosphoproteomic and metabolomic analyses we uncovered a possible glutathione deficiency and induction of oxidative stress in LMPTP KO cells that would explain the role of LMPTP in prostate cancer progression. Our findings implicate LMPTP in prostate cancer progression which taken together with our confirmation that loss of LMPTP responds synergistically with current prostate cancer drugs establishes LMPTP as a potential drug target for prostate cancer patients.

INTRODUCTION

Globally, prostate cancer is the second-most diagnosed cancer in males with over a million new cases a year[1]; therefore, understanding the mechanism and progression of prostate cancer is vital in ongoing cancer research. Cancer progression, itself, is characterized as the rogue ability of cells in an organ to proliferate uncontrollably, evade death, and migrate to other sites thus spreading their lethal influence[2]. These basic cellular processes, like growth, survival and migration, depend on numerous cell-signaling cascades working simultaneously[2]. Alterations in these cascades, such as development of point mutations that result in constitutively active or inactive proteins, can cause irreparable changes, including cancer[2,3]. With cancer cells, signaling cascades that allow for growth and survival are typically favored while those that enforce cell death and DNA repair tend to be inactivated.[2]

Pertinent to cell signaling cascades and cellular process regulation are post-translational modifications made on proteins after initial translation has occurred, such as glycosylation, methylation, and phosphorylation[3,4]. Phosphorylation of proteins on serine, threonine, or tyrosine residues can reversibly activate or inactivate the target proteins which in turn activates or inactivates various pathways[4,5]. Two classes of proteins work together to ensure proper cellular function via phosphorylation regulation — kinases and phosphatases[4]. Kinases catalyze the addition of a phosphate group to a protein while phosphatases catalyze the removal of said phosphate group[4]. Because kinases and phosphatases contribute greatly to signaling cascades and cellular functions, balancing the expression of kinases and phosphatases is vital to maintaining normal cellular processes like growth and survival[4,5].

When the balance between kinase and phosphatase expressions is disrupted, cancer can develop[2]. Typically, unusual activation of kinases tends to promote uncontrolled cell growth, leading to cancer [4,5]. These kinases are given the name oncogenes because their activation results in cancer[4]. On the other end of the spectrum, inactivation of many phosphatases has been linked to cancer progression because, when functional, phosphatases typically turn off growth and survival pathways[6]. As a result, most phosphatases are termed tumor suppressors[6]. Oncogenes have been the center of targeted drug therapies because small molecule inhibitors can be synthesized to block the function of an overexpressed or hyperactivated protein[5]. With tumor suppressors, corrected copies of the mutated protein would need to be delivered to specific cancer cells in the body and expressed at the right time, for the right duration, and at the right levels[7]. Consequently, there have been fewer phosphatase drug targets when it comes to cancer[6].

Although historically categorized as tumor suppressors[6], more protein tyrosine phosphatases (PTPs) have emerged as candidate oncogenes, such as the Src homology domain containing phosphatase 2 (SHP2)[8]. Another reported oncogenic PTP is our protein of interest, the low-molecular-weight protein tyrosine phosphatase (LMPTP)[9]. As implied by its name, LMPTP is a small (18 kDa) PTP encoded by the acid phosphatase 1 (*ACP1*) gene[9]. The ubiquitously expressed LMPTP has been identified as a potential biomarker upregulated in patients with hormone-naïve metastatic prostate cancer, the most deadly and progressive form of prostate cancer[10]. The same clinical study established a negative correlation between patient prostate cancer-free survival and LMPTP expression[10]. These findings posit LMPTP as a

potentially valuable target for prostate cancer progression. While it is the second-most prevalent cancer in males, prostate cancer progression tends to be slower and less aggressive when localized to the prostate and responsive to androgen therapy[1]. Once the cancer has metastasized to the surrounding bone, survival rates are significantly decreased, making therapeutics less effective[1]. Therefore, this paper aims to dive deeper into the role of LMPTP in prostate cancer growth and metastasis in hopes of providing a novel candidate for drug therapy.

First, we confirmed the oncogenic nature of LMPTP in prostate cancer proliferation through a series of *in vitro* and *in vivo* assays using CRISPR-Cas9 generated LMPTP knockout prostate cancer cell lines. Additionally, we reproduced our *in vivo* results of impaired prostate tumor growth using an orally bioavailable LMPTP inhibitor developed by our lab[11]. Next we designed a series of *in vitro* and *in vivo assays* that mimicked various steps in metastasis to implicate LMPTP in metastatic development. These assays included an (1) *in vitro* tumorigenesis assay that tested the ability of the prostate cancer cells to colonize and form solid tumors, (2) *in vitro* invasion assay to mimic the invasion and migration through the extracellular matrix, and (3) *in vivo* intraosseous injection to observe the ability to colonize in bone. Our findings suggested that LMPTP promotes prostate cancer proliferation, tumorigenesis, invasion, and bone growth. We are concurrently employing phosphoproteomic and metabolomic analysis to unravel the molecular mechanism by which LMPTP promotes prostate cancer growth and metastasis to better understand its relevance in prostate cancer therapeutics.

Materials & Methods

TCGA Analysis

Prostate adenocarcinoma (PRAD) data regarding *ACP1* expression and patient survival outcomes were taken from the UALCAN web-portal[12]. The UALCAN web-portal was programmed and designed to quickly analyze the larger scale cancer genomic data generated by The Cancer Genome Atlas (TCGA) project.

Cell Culture and Reagents

Mouse Myc-CaP prostate cancer cells (a gift from Dr. Charles Sawyers) were grown in Dulbecco's minimal essential medium (DMEM) supplemented with 10% fetal bovine serum (FBS) and 100 U/mL penicillin & 100 µg/mL streptomycin (1x Pen/Strep). Human C4-2B prostate cancer cell lines purchased from ATCC were grown in Roswell Park Memorial Institute 1640 medium (RPMI 1640) supplemented with 10% FBS and 1x Pen/Strep. All cells were maintained in a sterile incubator at 37°C and 5% CO_2. During serum starvation treatments, cells 10% FBS media was swapped for 0.1% FBS media for the indicated duration of starvation. For growth inhibition assays, Docetaxel and Cabazitaxel (Selleckchem) were reconstituted using DMSO and aliquoted at varying concentrations. Cells undergoing Docetaxel or Cabazitaxel treatment were treated with serum starved media containing the drug.

LMPTP Knockout (KO) Generation

gRNA design

The guide RNA (gRNA) targeting Exon 1 of the *ACP1* locus was selected from the CRISPR gRNA Design tool found on ATUM.bio which identified gRNA options within a given genomic DNA (gDNA) sequence ranked by order of target specificity. The

gRNA was inserted into a pD1301-plasmid expressing the Cas9 endonuclease, a kanamycin resistance sequence for bacterial selection, and a GFP coding sequence for mammalian selection by ATUM.

Plasmid amplification and extraction

E.coli stab containing the Cas9- gRNA plasmid was then streaked onto agar with kanamycin at a working concentration of 50µg/mL. After growth overnight, a single colony was used as starter culture and placed in 7 mL LB medium with kanamycin for 6-8 hours in a bacterial shaker incubator at 37°C. The starter culture was diluted 1:1000 into 300 mL of LB medium and grown for 12-16 hours in a bacterial shaker incubator at 37°C. After which, the plasmid was extracted using a Plasmid MaxiPrep kit from QIAGEN following the manufacturer's instructions. Final plasmid concentration was measured using a Nanodrop.

Transfection and cell sorting

Myc-CaP and C4-2B cells were grown in 6-well plates and transfected at about 50-60% confluency with 500 ng plasmid DNA using the Lipofectamine 3000 kit (Life Technologies) following the manufacturer's instructions. Two days after transfection, cells were trypsinized, neutralized with DMEM, and resuspended in ice cold FACS buffer (25 mM HEPES. 1mM EDTA, 1% FBS in PBS). GFP+ Myc-CaP or C4-2B cells, indicative of successful plasmid uptake, were single- sorted into 96 well plates containing DMEM or RPMI media with 10% FBS and Pen/Strep.

LMPTP KO clone characterization

Plates were monitored twice a week for colony formation. When the colony reached about 0.5 mm in diameter, colony was passaged to a larger well plate. The

passaging scheme ran as follows: 96 well plate to 24 well plates to 6 well plates to 10 cm plates to 15 cm plates for freezing down. During the growing of the CRISPR clones, gDNA was also isolated for sequencing or Western blotting of LMPTP to confirm a successful knockout clone.

Western blotting

Cell lysis and harvest

Prostate cancer cells were lysed using 1x Cell Lysis Buffer (Cell Signaling Technology) with 1μM phenylmethylsulphonyl fluoride in deionized (DI) water. Lysates were kept cold (on ice or at 4°C) for the duration of the lysis. Samples were collected and sonicated for a total of 3 min and 45 sec pulsing for 15 sec on and 45 sec off. After sonication, samples were centrifuged for 30 min at max speed, and the supernatant containing the protein lysate was collected and quantified using the Pierce BCA Protein Assay kit (ThermoFisher).

SDS-PAGE

Equal amounts of proteins, ranging from 25- 50 μg protein/sample, were loaded onto 4-20% pre-cast Tris-Glycine gels (Invitrogen). Samples were prepared with protein lysates, 2x or 6x Laemmli SDS Sample Buffer containing 5% beta-mercaptoethanol, and DI water adjusted to the final volume. SDS-PAGE ran for 1.5 hours at 120 V or until sample buffer reached to bottom of the gel.

Transfer and Western Blotting

Proteins were transferred from SDS-PAGE to a 0.45 μm nitrocellulose membrane using a wet transfer method. Proteins transferred at 0.4 mA for 45 min to 1.5 hr in transfer buffer containing 1x running buffer and 20% methanol. Membranes were

blocked with 5% BSA in TBS-T with NaN_3 for 1 hr at room temperature. After blocking, membranes were left in primary antibodies (Abs) in 5% BSA in TBS-T with NaN_3 overnight on rocker in the cold room (4°C). Primary Ab was removed, and membrane were washed 3 times with TBS-T for 10 min each before adding the secondary Ab in 5% dry milk in TBS-T for up to 1 hr. Membranes were then washed with TBST-T 3 times for 10 min before developing. Crescendo Western HRP substrate (Millipore Sigma) was added to membrane for 2-5 minutes prior to imaging using GeneSys G-Box. Quantification of protein levels was performed using the ImageJ software.

Cell Proliferation Assay

Wild-type (WT) and LMPTP KO prostate cancer cell lines were plated in triplicate at equal counts into 12 well plates. Cells were left to grow for 5 days undisturbed except for replenishing the media three days in. After 5 days of growth, cells were fixed with 70% ethanol and stained with 0.05% Crystal Violet (in 25% ethanol). Plates were gently rinsed with DI water and left to dry overnight away from light. Crystal violet was extracted using Sorenson's extraction reagent (50 mM sodium citrate & 50 mM citric acid dissolved in 50% ethanol). Extracted solution was diluted anywhere between 1:2 and 1:10 to determine. Diluted samples were added to a flat, transparent 96-well plate in triplicate and absorbance was read at 595 nm using a Tecan plate reader.

Xenograft Mouse Model

7- to 8-week-old severe combined immunodeficient (SCID) mice were injected subcutaneously along their right and left dorsal flanks with 200K WT or LMPTP KO Myc-CaP cells suspended in 50% Matrigel Matrix Phenol Red Free (BD, #3562377) and 50% DMEM at a final volume of 100 µL. Tumor length, width, and depth were

measured using a caliper starting 7 days after initial inoculation for 3 times a week to calculate tumor volume. Mice were also weighed during the duration of the study. Study endpoint was defined as when the tumor reached 2 cm in diameter or the mouse lost 20% of its initial body weight. Mice were sacrificed using a CO_2 chamber and according to the IACUC protocol. Mice in the LMPTP inhibitor compound study were injected with 200K WT Myc-CaP cells and tumor volumes were recorded starting at 7 days. Two weeks after the initial injection, half the mice were placed on chow formulated with 1% w/w Compd. 23 while the other half stayed on regular chow. Tumor monitoring was performed the same way as the LMPTP KO study.

Soft Agar Colony Formation Assay

A 1:1 ratio of 1.2% w/w noble agar (VWR, 90000-772) to 2X DMEM or RPMI media was plated on the bottom of 6 well plates. After solidification of the bottom layer, prostate cancer cells suspended in a 1:1 mixture of 0.6% noble agar to 2X DMEM or RPMI media were plated on top. Myc-CaP and C4-2B cells were plated at 35K cells/well and 20K cells/well, respectively. After solidification of the top layer, a bit of 10% FBS in 1x media was added each well to prevent gel agar from drying. Plates were placed in the 37°C incubator for 21 days while maintaining a thin layer of 10% FBS in 1X media. Colonies were stained with crystal violet, washed, and imaged using the AxioVert Marianas Microscopy System. Images were captured as Z-stacks and compiled into one using ImageJ.

Matrigel Invasion Assay

WT and LMPTP KO prostate cancer cells were serum starved overnight (18 hours) in DMEM or RPMI media containing 0.1% FBS with Pen/Strep. Starved cells

were placed in the top chamber of a Matrigel Invasion Chamber (Corning, 354480) with the bottom chamber containing DMEM or RPMI media with 10% FBS with Pen/Strep to promote migration. Two days later, cells on the bottom of the transwells were fixed with 100% methanol and stained using 0.05% crystal violet in 25% ethanol.

Intraosseous Mouse Model

Three days prior to the procedure, mice were split into separate cages with either regular chow or chow formulated with 1% w/w Compd. 23. On the day of the injection, mice were anesthetized with isoflurane using a nosecone set up. 100K Luciferase-expressing Myc-CaP (Luc-Myc-CaP) cells resuspended into 20µL ice cold PBS were injected into the left tibia of SCID mice between 8-10 weeks old. One week following the procedure, mice were injected with 150 mg Luciferin/kg body weight and imaged using an *in vivo* imaging system (IVIS). Pierce D-Luciferin Monopotassium Salt was purchased from ThermoFisher and reconstituted using PBS. Images obtained from the IVIS were processed and quantified using the Aura Imaging Software.

Phosphoproteomic Analysis

Phosphoproteomic sample preparations

WT and LMPTP KO prostate cancer cells were grown in triplicate in 15 cm plates overnight in media containing 10% FBS with Pen/Strep. Cells were then lysed in 8 M urea, collected, and snap frozen. Myc-CaP KO1, KO2, and KO4 along with C4-2B KO1, KO2, KO3, and KO4 were sent along with their respective WTs for analysis.

Phosphoproteomic analysis performed at the Kettenbach laboratory

Lysates were reduced, alkylated, digested to peptides and desalted prior to quantitative recovery of phosphopeptides using Fe-NTA columns (ThermoFisher).

Phospho-peptides from each condition will then be labeled with unique tandem mass tags (TMT), fractionated, and followed with high performance liquid chromatography with tandem mass spectrometry (LC-MS/MS). Phosphopeptide ratios were calculated as KO/WT and log-transformed and p-values will be calculated by two-tailed Student's t-test. Canonical pathway analysis of phosphoproteins displaying log2(LMPTP KO/WT signal ratio) <-0.59 or >0.59 and p-value <0.05 were performed using the Core Analysis function in the Ingenuity Pathway Analysis (IPA) platform.

Metabolomic Analysis

Metabolomic sample preparations

WT and LMPTP KO prostate cancer cells were grown in five replicates in 15 cm plates overnight the same was as prepared for phosphoproteomic analysis. For sample collection, the extracellular metabolome (media) along with intracellular metabolome (cell pellet) were retained and snap frozen. Here, WT and LMPTP KO1 Myc-Cap cells and WT and LMPTP KO1 C4-2B cells were sent for analysis because both KO lines had the most robust growth phenotype.

Metabolomic analysis performed at the Tiziani laboratory

Assessment of the intracellular metabolome was performed by untargeted polar and targeted nonpolar ultrahigh performance liquid chromatography coupled to mass spectrometry (UHPLC-MS) by our collaborators at the Tiziani Lab at The University of Austin Texas.

GSH/GSSG-Glo Detection Assay

WT and LMPTP KO prostate cancer cells were grown in normal cell culture conditions to 80% confluency then harvested using trypsin. Glutathione assay was

performed using GSH/GSSG-Glo assay (Promega, V6611) according to the manufacturer's instructions. Samples were run in duplicate on opaque, white 96- well plates (Sigma). Bioluminescence was read using a Tecan plate reader.

RESULTS

High LMPTP expression in prostate adenocarcinoma (PRAD) patients correlates negatively with survival time

Beginning in 2006, the National Cancer Institute and the National Human Genome Research Institute initiated a large-scale cancer genomic analysis effort known as The Cancer Genome Atlas (TCGA) program to better characterize and understand the molecular basis of 33 cancer types from 20,000 patient samples. Researchers from the University of Alabama at Birmingham developed the UALCAN interface to combine transcriptomic or genomic results with clinical patient outcomes[12]. Using the UALCAN interface, we found that *ACP1* expression, the gene encoding LMPTP, is slightly but significantly increased in prostate tumor tissues compared to normal, non-cancer samples by approximately 10% **(Figure 1A).** Furthermore, high expression of *ACP1*—defined as patients within the upper quartile of PRAD *ACP1* expression—correlated with lower survival probability over a span of ten years **(Figure 1B)**. This negative correlation between LMPTP expression and patient survival posits LMPTP as a potential target for prostate cancer progression.

Generation and characterization of LMPTP knockout prostate cancer cells

To study the role of LMPTP in prostate cancer progression, we generated LMPTP knockout (KO) clones using CRISPR-Cas9 in two prostate cancer cell lines: the mouse Myc-CaP and human C4-2B. Myc-CaP cells were derived from the tumor of a transgenic mouse expressing the human *c-Myc* oncogene in the prostate, and C4-2B cells were derived from LNCaP cells as a bone metastatic subline. Wildtype (WT) Myc-CaP and C4-2B cells were transfected with a plasmid containing Cas9

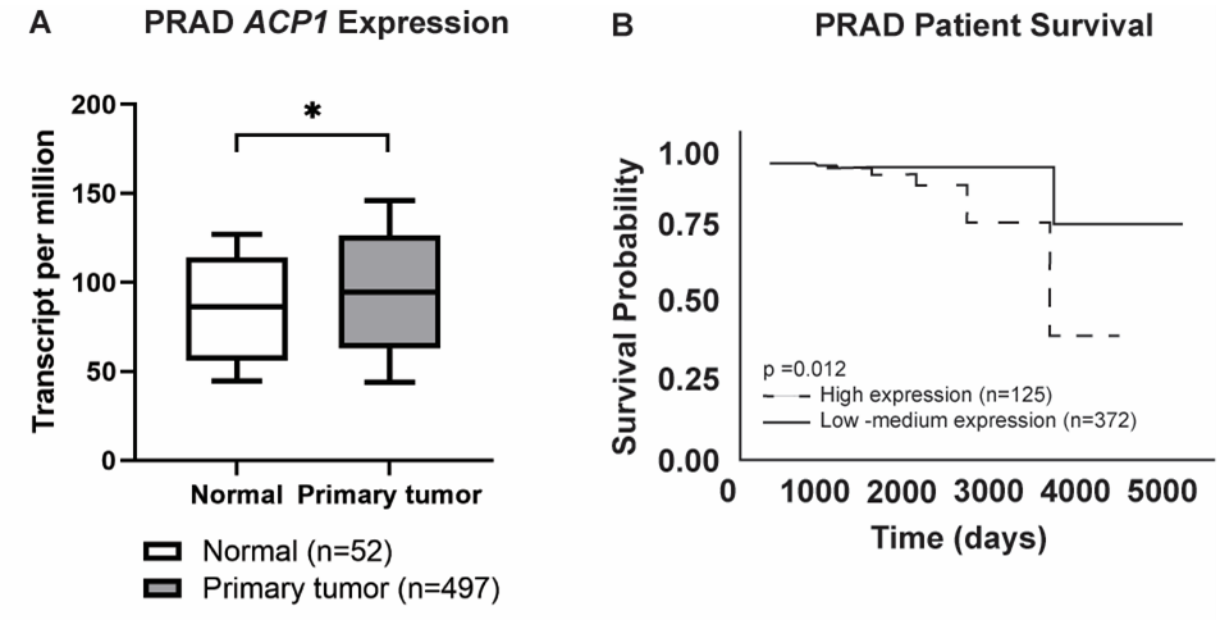

Figure 1: *ACP1* is upregulated in PRAD tumors and correlates negatively with patient survival. Genomic data derived from The Cancer Genome Atlas (TCGA) project were processed through the UALCAN interface to study *ACP1* expression in PRAD patients. **(A)** Differences in *ACP1* expression were observed between normal and primary prostate tumor tissues from TCGA RNA sequencing data. Significance was determined on UALCAN using a statistical T-test,* p=0.0084. **(B)** Kaplan Meier curve comparing survival probability of patients with high to low/moderate *ACP1* expression. Significance was determined on UALCAN using a log-rank test.

endonuclease, a guide RNA targeting the *ACP1* locus with minimal off-target effects, and a GFP-selection marker. After transfection, single-cell GFP+ prostate cancer cells **(Figure 2 A-B)** were sorted into 96-well plates to grow and characterize for potential LMPTP knockouts. Characterization of these KO lines consisted of gDNA sequencing to identify exact insertion or deletion mutations and Western blotting to confirm loss of LMPTP protein expression **(Figure 2 C-D)**. From here, we selected three Myc-CaP LMPTP KO lines (KO1, KO2, and KO4) and four C4-2B LMPTP KO lines (KO1, KO2, KO3, and KO4) to study further **(Figure 2 C-D)**.

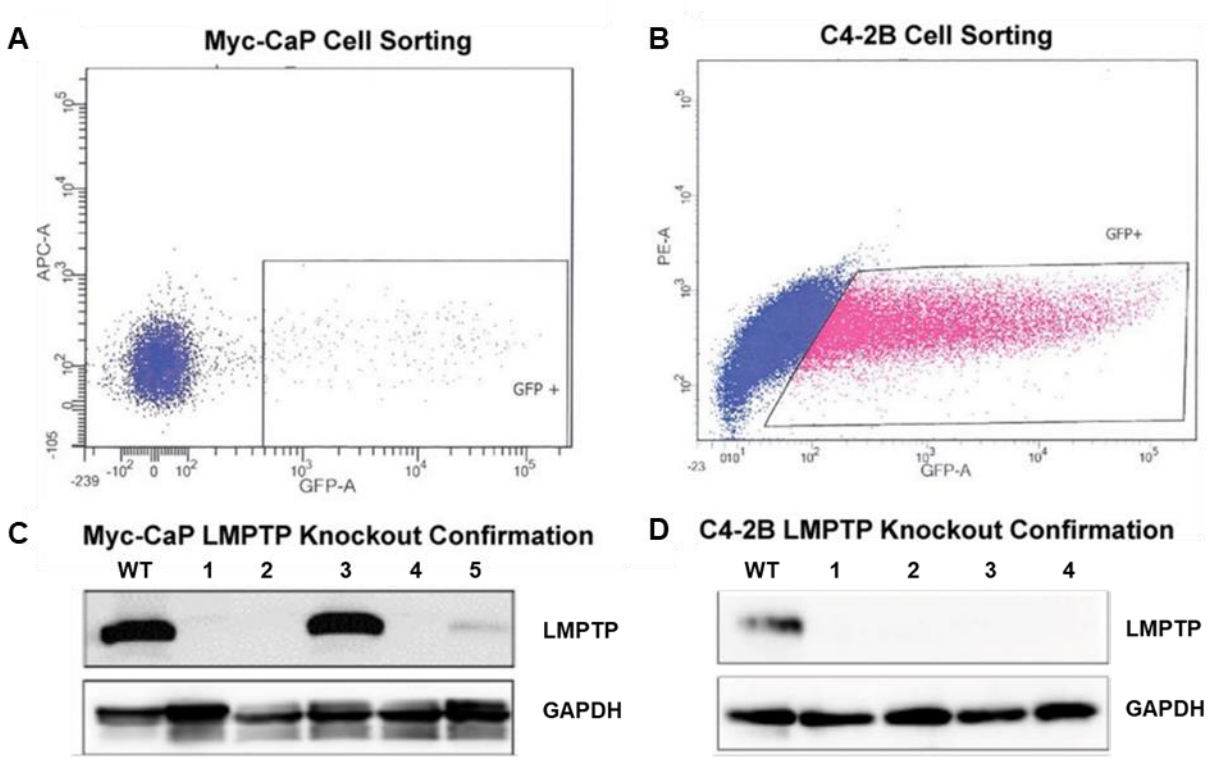

Figure 2: Generation of LMPTP KO prostate cancer cells using CRISPR-Cas9. Wildtype (WT) mouse Myc-CaP or human C4-2B cells were transfected with plasmids containing the Cas9 endonuclease, a gRNA targeting the *ACP1* locus, and a GFP-selection marker. **(A-B)** After transfection, GFP+ prostate cancer cells were sorted into 96-well plates, grown, and characterized. **(C-D)** Confirmation of LMPTP KO clones via western blotting. *This figure is coauthored by Joseph Chang and Tiffany Nguyen. Joseph Chang and Tiffany Nguyen are the primary authors for this figure and contributed equally.*

LMPTP promotes prostate cancer growth *in vitro* and *in vivo*

After confirming several LMPTP KO clones in both Myc-CaP and C4-2B prostate cancer cell lines, we used an *in vitro* growth assay to compare the proliferation rates of these LMPTP KO clones to its respective WT. Equal amount of both WT and LMPTP KO prostate cancer cells were plated and left to growth undisturbed for five days. After the growth period, we found that LMPTP KO cells grew slower than the WT cells **(Figure 3)**. LMPTP KO Myc-CaP clones all grew at a rate less than 65% relative to the WT Myc-CaP cells with KO1 growing at only approximately 45% of the WT **(Figure 3A).**

Similarly, LMPTP KO C4-2B clones all grew at a rate less than 60% of the WT C4-2B cells with KO1 and KO2 growing at only 41% and 44%, respectively **(Figure 3B)**.

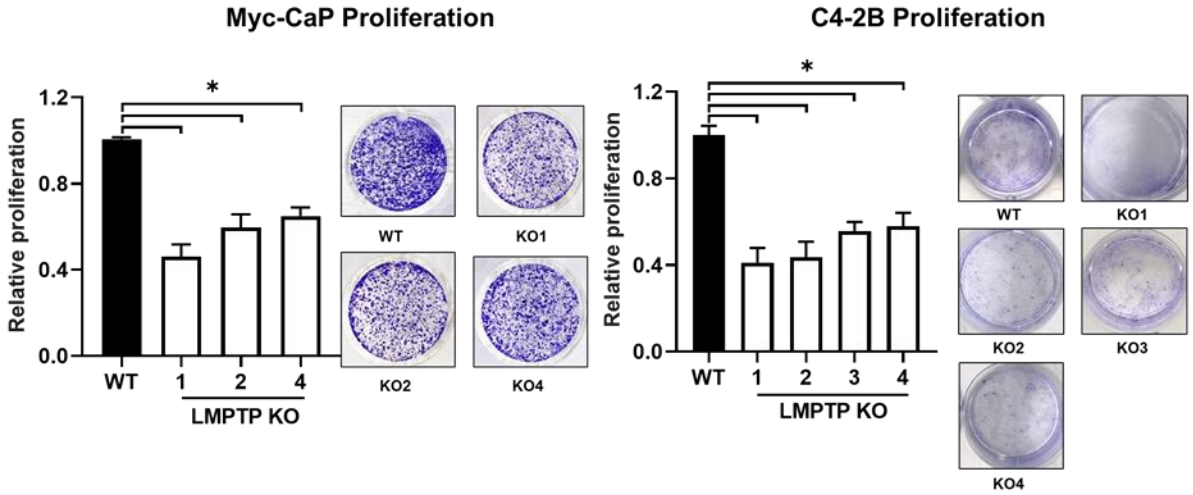

Figure 3: Loss of LMPTP impairs prostate cancer cell growth in *vitro*. (A-B) WT and LMPTP KO **(A)** Myc-CaP and **(B)** C4-2B cells were plated and left to grow. After five days cells were fixed and stained with crystal violet. Stain was extracted and read at 590 nm to quantify proliferation relative to the WT growth condition. **(A-B)** Mean±SEM relative proliferation from four independent experiments shown with representative images. *, $p<0.05$, Mann-Whitney test. *This figure is coauthored by Joseph Chang and Tiffany Nguyen. Joseph Chang and Tiffany Nguyen are the primary authors for this figure and contributed equally.*

Next, we sought to observe the proliferative effects of LMPTP *in vivo* by using a subcutaneous tumor xenograft model in both an LMPTP knockout and inhibitor study. WT and LMPTP KO Myc-CaP cells were injected into SCID mice. Tumor volumes were measured using a caliper three times a week over the span of 30 days, and the endpoint was defined as when the length of the tumor reached 2 cm in diameter. At the end of the 30 days, the WT tumors grew on average twice the size of the LMPTP KO tumors **(Figure 4A).** Moreover, the WT tumors reached the defined endpoint much sooner than the LMPTP KO tumors with only one mouse remaining after 35 days

compared to the five LMPTP KO inoculated mice **(Figure 4B)**. The longest surviving LMPTP KO tumor mouse reached the defined endpoint at day 52, which is 15 days longer than the longest surviving WT tumor mouse **(Figure 4B)**. Next, we used a similar xenograft model to observe whether inhibiting LMPTP catalytic activity affects prostate tumor growth. WT Myc-CaP cells were injected into SCID mice. Two weeks following the procedure, mice were placed on regular chow or chow formulated with 0.1% w/w Compd. 23, an LMPTP inhibitor developed in our lab[11]. Like our LMPTP KO study, we found that inhibition of LMPTP delayed tumor growth **(Figure 4C).** Taken together, the results from **Figure 3** and **Figure 4** indicate that LMPTP promotes prostate cancer cell growth.

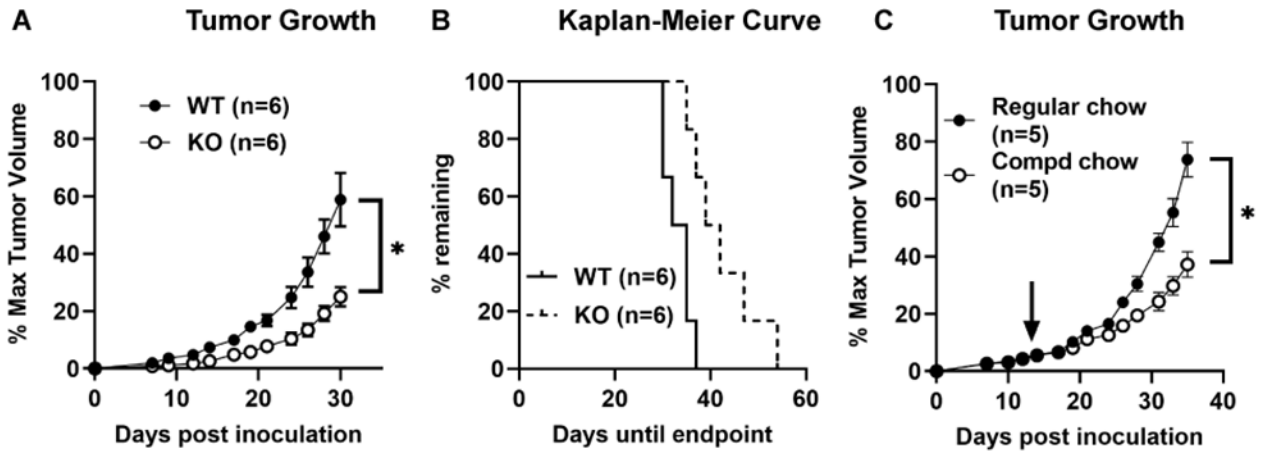

Figure 4: Loss or inhibition of LMPTP impairs prostate tumor growth in mice. (A-B) SCID mice were injected subcutaneously with WT or LMPTP KO Myc-CaP cells suspended in Matrigel. Tumor volumes were measured with a caliper for 30 days, and the endpoint was determined when tumors reached 2 cm long. **(A)** Mean±SEM % max tumor volume. **(B)** Kaplan-Meier curve of mice from (A). p=0.0083, Gehan-Breslow-Wilcoxon test. **(C)** Tumor volumes of mice inoculated with WT Myc-CaP cells. After 14 days, mice were placed on regular chow or chow formulated with 0.1% w/w LMPTP inhibitor Compd. 23. Mean±SEM % max tumor volume. **(A, C)** *, p<0.0001, 2-way ANOVA. *This figure is coauthored by Joseph Chang, Michael Diaz, and Tiffany Nguyen. Tiffany Nguyen is the secondary author for this figure.*

LMPTP supports metastatic characteristics including tumorigenesis, invasion, and tumor growth in bone

After establishing LMPTP as positive driver of prostate cancer proliferation, we sought to identify its role in the progression towards metastasis. One key process in metastasis is the ability to colonize and grow in a new site; therefore, we sought to assess how loss of LMPTP affects tumorigenesis—the initial formation of a tumor—through a soft agar colony formation assay. The formation of tumors relies heavily on anchorage independent growth, which is the ability of cancer cells to grow without anchoring to a solid surface, such as the basement membrane or neighboring cells[13]. To mimic a system lacking a solid surface, we suspended prostate cancer cells, Myc-CaP or C4-2B, in a soft agar solution and plated the mixture of cells on top of denser soft agar. Colonies were left to grow for 21 days before staining, counting, and imaging five random fields. In both the Myc-CaP (**Fig. 5A**) and C4-2B (**Fig. 5B**) cells, there was more colony growth per imaged frame in the WT lines compared to the different CRISPR-generated KO clones (**Fig. 5**). Ultimately, the results show that loss of LMPTP in both Myc-CaP and C4-2B inhibits colony formation on soft agar, which is relevant towards both primary tumor growth and tumor growth at a metastatic site.

Another important step in metastasis is the ability of a cancer cell to degrade the extracellular matrix and migrate away from the primary tumor towards vasculature[14]. This ability is often known as invasion[14], and we used a Matrigel invasion chamber assay to model prostate cancer cell invasion *in vitro*. Prostate cancer cells were serum-starved in 0.1% FBS the night prior then added to the top of a Matrigel-coated chamber well. Underneath the well was 10% FBS media as a chemo-attractant to

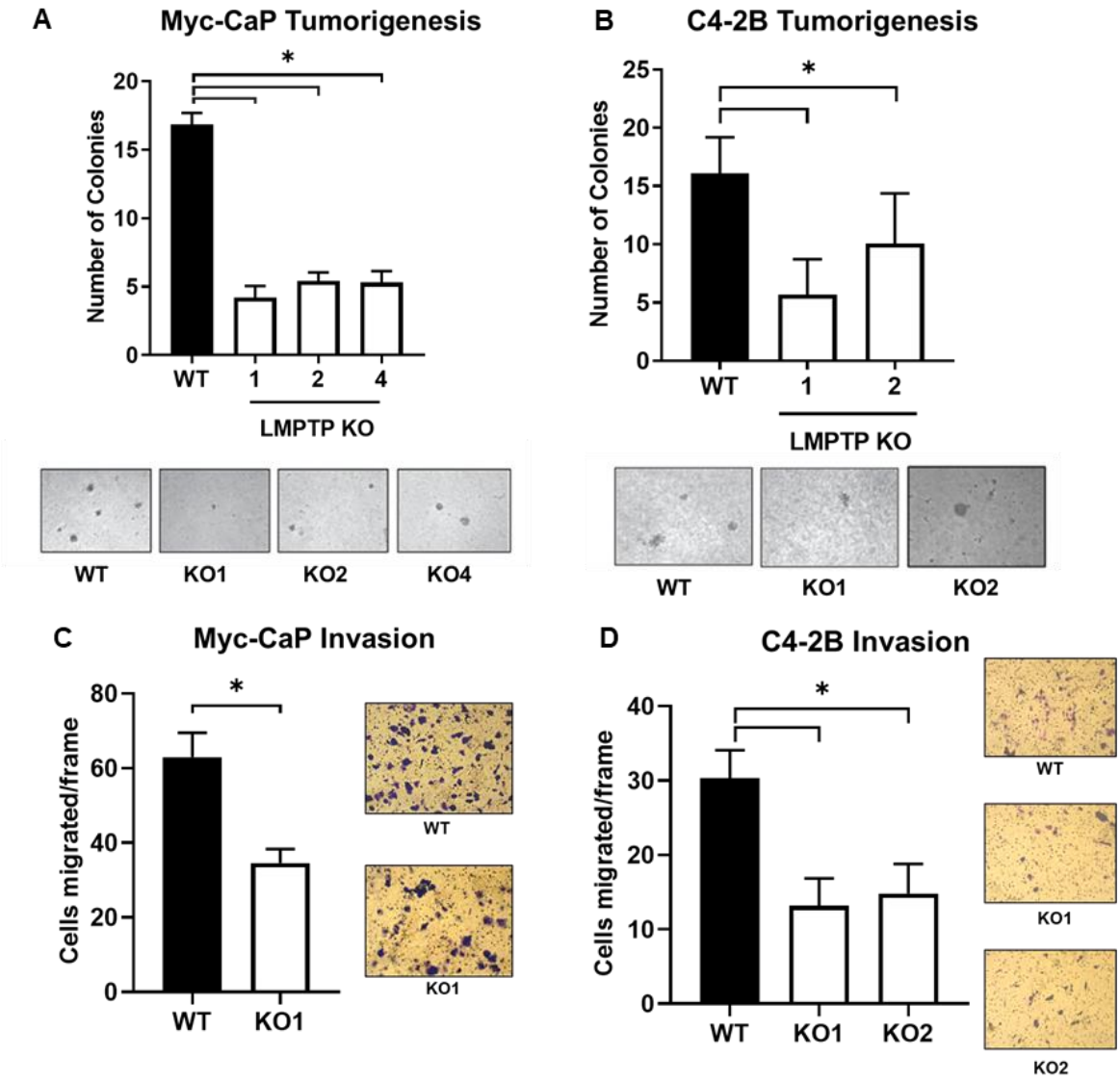

Figure 5: Loss of LMPTP impairs metastatic characteristics in prostate cancer cells. **(A-B)** WT or LMPTP KO prostate cancer cells were seeded on noble agar for a tumorigenesis assay. After 21 days, colonies were stained with crystal violet and counted from five random frames. **(C-D)** WT or LMPTP KO cells were starved overnight in 0.1% FBS then seeded on top of Matrigel-coated transwells for an invasion assay. The lower chambers contained 10% FBS to promote migration. After two days migrated cells were fixed, stained with crystal violet, and counted. **(A,C)** Mean±SEM from four independent experiments done with Myc-CaP cells with significance determined by the Mann-Whitney test *, $p < 0.05$. **(B,D)** Mean±SEM from three independent experiments done with C4-2B prostate cancer cells. Significance determined by the unpaired t-test is denoted by *, $p < 0.05$. Representative images of each assay shown. *This figure is coauthored by Joseph Chang and Tiffany Nguyen. Tiffany Nguyen is the primary authors for this figure.*

promote the invasion and migration of the starved cancer cells through the extracellular-like Matrigel matrix, into the bottom chamber. After two days of migration, cells on the bottom chamber were fixed and stained in crystal violet to count. The LMPTP KO Myc-CaP cells invaded about half as much as the WT Myc-CaP cells **(Figure 5C)**. Similarly, the C4-2B KO clones KO1 and KO2 invaded about 43% and 49% as much as the WT C4-2B cells, respectively **(Figure 5D)**. Altogether, we saw that LMPTP promotes prostate cancer tumorigenesis on soft agar and invasion through a Matrigel matrix, suggesting its potential role in metastatic development. However, there was no difference observed between the WT and LMPTP KO prostate cancer cells when it came to a transendothelial migration assay modeling the entry into blood vessels known as intravasation (data not shown)[14].

Because the most common site of prostate cancer metastasis is the bone, we used an intraosseous injection mouse model to observe bone tumor colonization and growth. Here mice were placed on regular chow or chow formulated with 0.1% w/w LMPTP inhibitor Compd. 23[11] three days prior to the procedure. On the day of procedure, WT Luciferase-expressing Myc-CaP (Luc-Myc-CaP) cells were injected into the left tibia of SCID mice leaving the right tibia for a bioluminescent background control. Tumor growth was measured up to two times a week using luciferin injections and an IVIS spectrum. Our preliminary data showed that tumors in mice placed on the inhibitor chow started out much slower than those placed on the regular chow and the difference continued to separate as time went on **(Figure 6)**. While the results are promising, we are currently repeating the experiment to more thoroughly assess the role of LMPTP in prostate tumor bone metastasis.

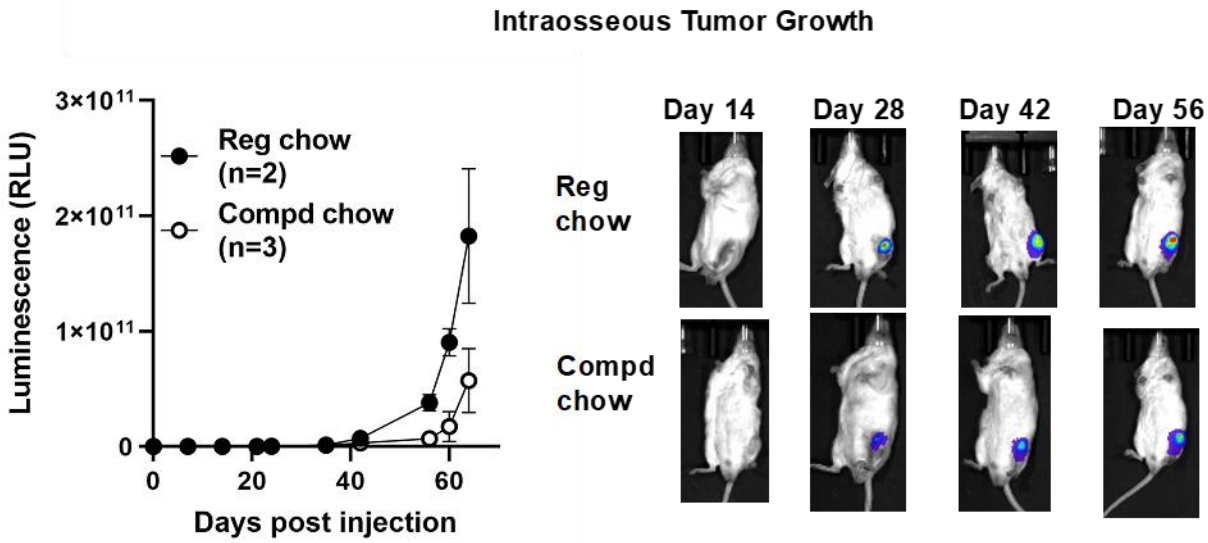

Figure 6: Inhibition of LMPTP impairs prostate tumor bone growth *in vivo*. Three days prior to the procedure, SCID mice were placed on regular chow or LMPTP inhibitor-formulated compound chow. Luciferase expressing Myc-CaP cells were injected into the left tibia of SCID mice and left to grow. After initial injection, mice were injected with luciferin and imaged using the IVIS system up to two times a week to monitor tumor growth. **(A)** Mean±SEM luminescent intensity measured over 10 weeks. **(B)** Representative images of tumor growth at indicated time points.

Elucidating the molecular mechanism by which LMPTP promotes prostate cancer progression

After demonstrating that LMPTP promotes prostate cancer growth and metastasis through a series of *in vitro* and *in vivo* experiments, we sought to uncover the molecular mechanism that would explain these observed phenotypes. We first used phosphoproteomic analysis to identify potential LMPTP-related phospho-signaling networks in prostate cancer cells. WT and LMPTP KO cells were grown for 24 hours before lysis in urea and sent to our collaborators at the Kettenbach Lab at Dartmouth College. The phosphoproteomic analysis performed as described in **Figure 7A** revealed differences in phosphorylation levels of various phospho-proteins between

individual LMPTP KO prostate cancer cell lines and their respective WT counterparts. Inputting this data into the Ingenuity Pathway Analysis (IPA) platform, we were able to generate a list of most significantly different canonical pathways between the WT and LMPTP KO lines **(Figure 7B)**. Surprisingly, there was a lot of overlap in affected proteins between the top three canonical pathways—Molecular Mechanisms of Cancer, eukaryotic initiation factor 2 (eIF2) Signaling, and Insulin Receptor Signaling—that centered around eIF2 and eukaryotic initiation factor 4 (eIF4) signaling **(Figure 7B)**. To study the eIF2 signaling, a pathway that responds to stressors within the cell, we serum starved WT and LMPTP KO prostate cancer cells for 2 hours before blotting for eIF2 phosphorylation at site Ser51 (peIF2 S51)—an indication of pathway activation. We found that loss of LMPTP leads to hyper-activation of eIF2 signaling in response to serum starvation stress **(Figure 7 C-D)**. Next, we hope to dive deeper into how LMPTP regulates eIF2 signaling.

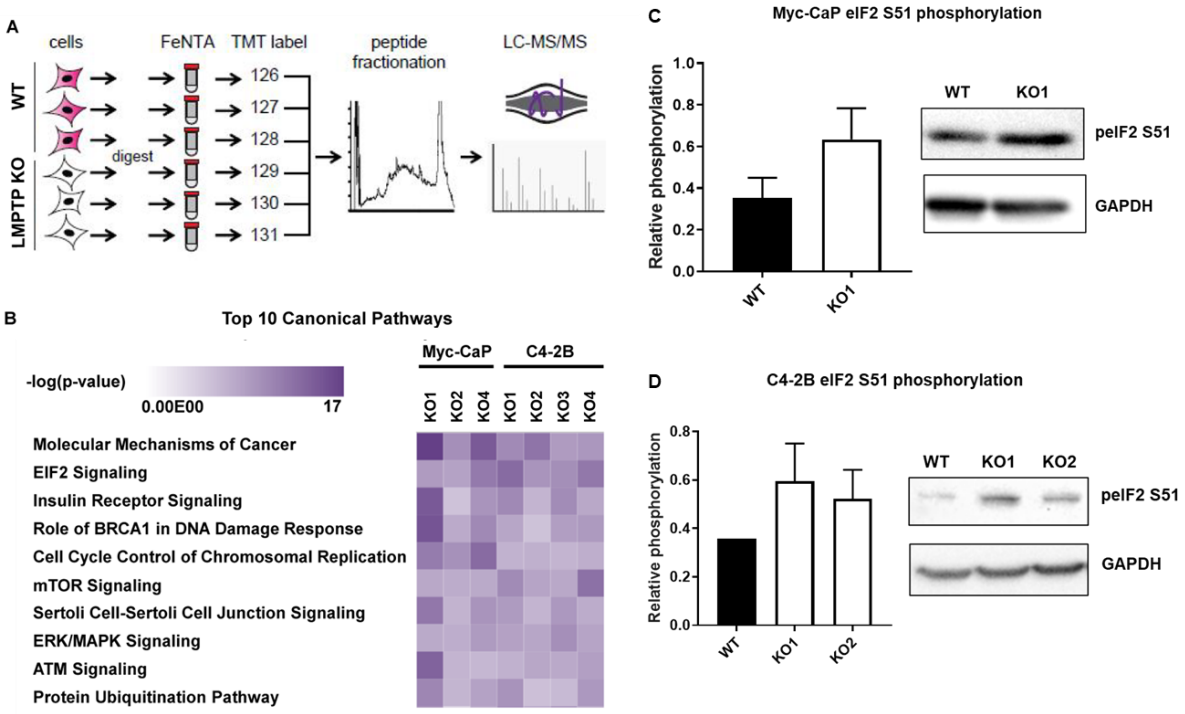

Figure 7: Phosphoproteomic analysis of prostate cancer cells identified eIF2 signaling as a potential molecular mechanism. (A) Scheme of phosphoproteomic analysis. **(B)** Heatmap demonstrating the most different canonical pathways between prostate cancer WT and LMPTP KO clones. Order is ranked from highest total score of –log (p-value). Analysis was performed using the IPA software. (C-D) eIF2 phosphorylation was assessed WT and LMPTP KO prostate cancer cells via western blotting in after 2 hours of serum starvation. Phosphorylation levels was quantified relative to GAPDH. Two independent experiments show with representative blots. *This figure is coauthored by Arminja Kettenbach and Tiffany Nguyen. Both authors contributed equally.*

Simultaneously, we also performed metabolomic analysis to identify key differences in the intracellular metabolic signatures of WT and LMPTP KO prostate cancer cells to shed light on the mechanism underlying the reduced proliferation in LMPTP KO cells. As such, WT and LMPTP KO cells were grown for 24 hours before pelleting to send to our collaborators at the Tiziani Lab at The University of Austin Texas. UHPLC-MS-based analysis was used to investigate the differences in the intracellular metabolome of WT and LMPTP KO prostate cancer cells, and PCA analysis indicated a striking difference between the WT and KO cells for both the Myc-CaP and C4-2B cell lines **(Figure 8A-B).** Furthermore, we noticed a significant

decrease in glutathione (GSH) levels in the Myc-CaP KO1 cell line compared to the WT Myc-CaP cells **(Figure 8 C);** however, glutathione levels were not detected in the C4-2B samples**.** We confirmed that glutathione levels are decreased in both LMPTP KO prostate cancer cell lines with a bioluminescent GSH assay designed by Promega **(Figure 8 D-E).** Altogether, the data suggests a glutathione deficiency in LMPTP KO cells.

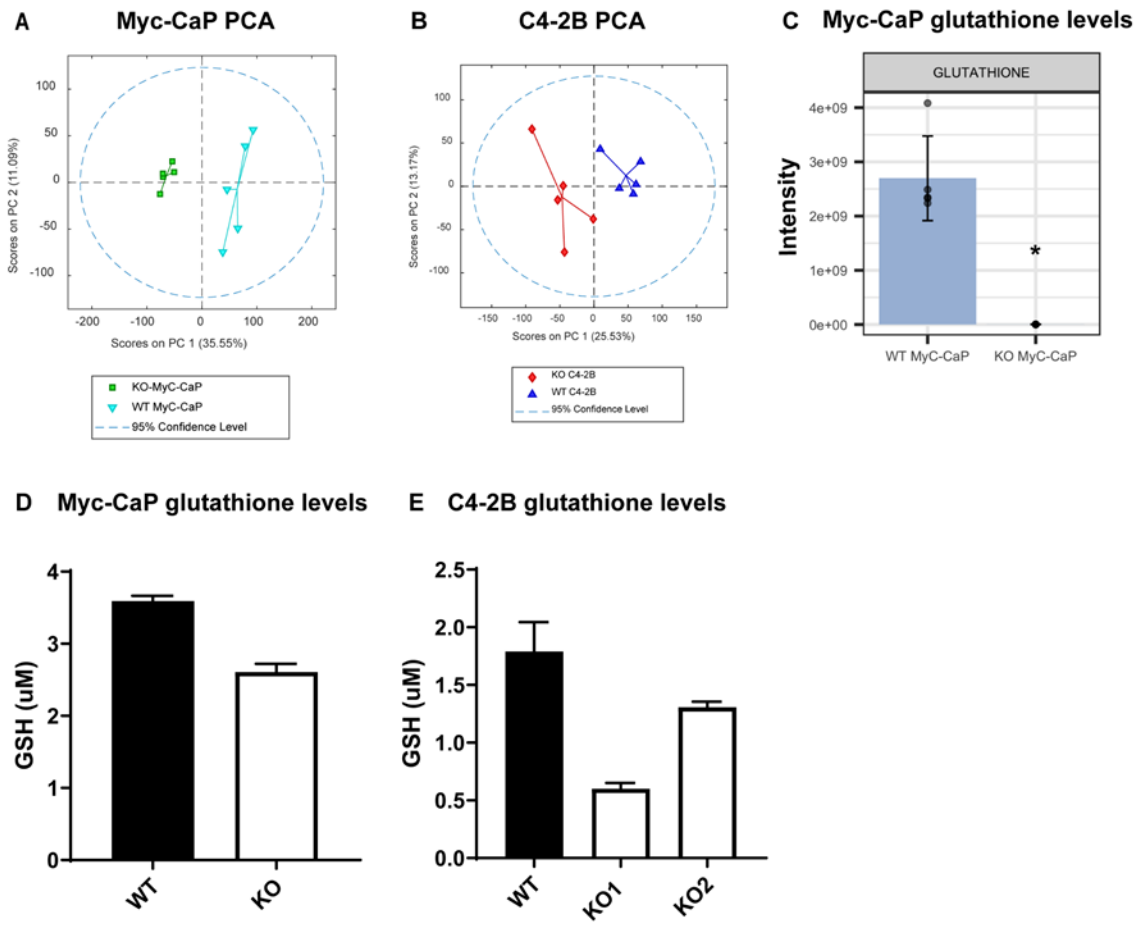

Figure 8: Metabolomic analysis of LMPTP KO prostate cancer cells reveals a decrease in glutathione levels. (A-B) PCA (PC1 vs PC2) obtained from the metabolomic analysis of WT and LMPTP KO prostate cancer cells. The intracellular metabolome was assessed by UHPLC-MS. **(C)** Intensity of glutathione levels in Myc-CaP WT and LMPTP KO cells normalized to the cell count. Mean ± SEM metabolite intensity from 5 biological replicates shown. **(D-E)** Basal glutathione concentrations in WT and LMPTP KO prostate cancer cells were detected using bioluminescent GSH detection assay. Data from independent experiments shown. *This figure is coauthored by Lavender Hackman, Stefano Tiziani, and Tiffany Nguyen. All authors contributed equally.*

Loss of LMPTP in conjunction with current prostate cancer therapeutics reduces proliferation even further

Our initial goal for this project was to investigate the role of LMPTP in prostate cancer progression with the hopes of positing LMPTP as a potential drug target. As

such, we wanted to confirm the pharmacological relevance of LMPTP. Using the *in vitro* growth assay, we compared the growth rate of WT and LMPTP KO Myc-CaP cells when treated with two common prostate cancer drugs, Docetaxel or Cabazitaxel. We found a synergistic effect between the loss of LMPTP and Docetaxel or Cabazitaxel treatment where LMPTP KO Myc-CaP cells grew even slower when combined with either drug **(Figure 10).** This data helps establish LMPTP as an option for combinatorial prostate cancer drug therapy.

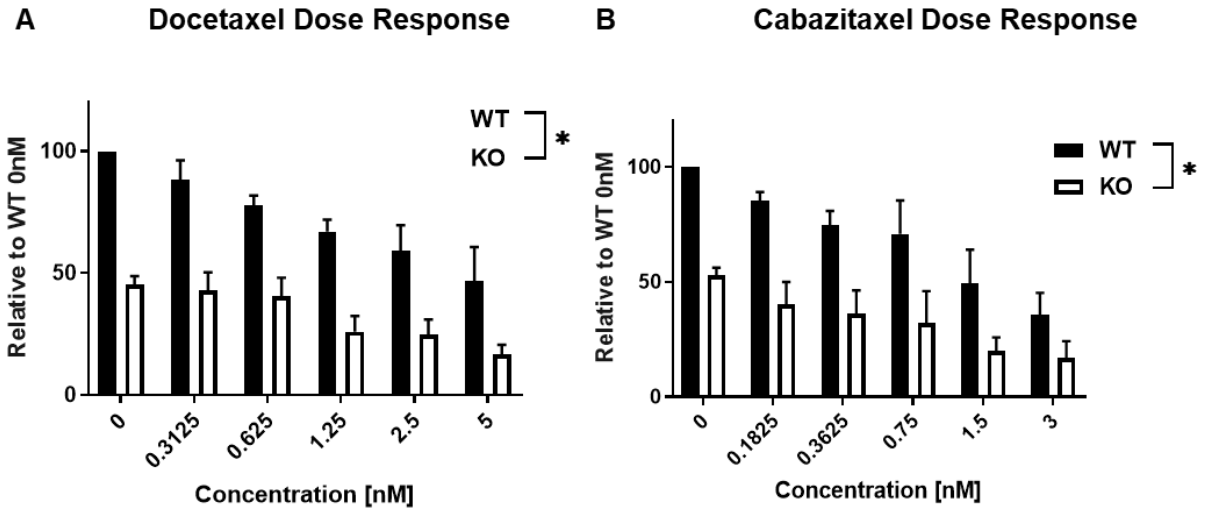

Figure 9: Loss of LMPTP synergizes with prostate cancer therapeutics. WT and LMPTP KO Myc-CaP cells were seeded into 12-well plates for a growth assay. After growing for 48 hours, cells were subjected to Docetaxel or Cabaxitaxel drug treatment at indicated concentrations and left to grow for an additional 72 hours. Growth was quantified as described in **Figure 3**. Mean±SEM relative proliferation from four independent experiments shown. *, $p<0.05$, 2-way ANOVA.

ACKNOWLEDGMENTS

Figures 2 and 3 are coauthored by Joseph Chang and Tiffany Nguyen. Both authors contributed equally.

Figure 4 is coauthored by Joseph Chang, Michael Diaz, and Tiffany Nguyen. Tiffany Nguyen is the secondary author.

Figure 5 is coauthored by Joseph Chang and Tiffany Nguyen. Tiffany Nguyen is the primary author.

Figure 7 is coauthored by Dr. Arminja Kettenbach and Tiffany Nguyen. Both authors contributed equally.

Figure 8 is coauthored by Lavender Hackman, Dr. Stefano Tiziani, and Tiffany Nguyen. All authors contributed equally.

DISCUSSION

Using two prostate cancer cell lines along with *in vitro* and *in vivo* assays, we showed evidence that LMPTP promotes prostate cancer growth and metastatic progression. One key hallmark of cancer is uncontrolled cell division and growth[2]. We established that prostate cancer cells without LMPTP grew at a much slower rate both in culture and in mice compared to WT LMPTP cells suggesting that LMPTP itself is a driver of prostate cancer proliferation. Furthermore, we used a soft agar colony formation assay to access the anchorage independent growth of WT and LMPTP KO prostate cancer cells. Anchorage independent growth allows tumors to grow to abnormally large sizes without restriction from environmental cues[2,13]. Additionally anchorage independent growth is also important for the initial formation of a tumor, a process known as tumorigenesis which is essential for both primary and secondary tumor formation[13,14].

Motivated by our tumorigenesis discovery, we sought to further assess the role of LMPTP in metastasis—another hallmark of cancer that is most commonly associated with prostate cancer-related deaths[1,2]. One early and essential step in cancer metastasis is the ability of a cancer cell within the primary tumor to break free and invade through the extracellular matrix[14]. We showed that LMPTP KO prostate cancer cell lines invaded and migrated through an *in vitro* Matrigel chamber migration assay much less than its WT counterpart. This suggests loss of LMPTP impaired the initial step of metastasis[14]. We were also able to study the last step of metastasis, which is the ability of prostate cancer cells to colonize the bone[14]—the most common metastasis site for prostate cancers. To do so, we developed an intraosseous injection mouse

model that tracked tumor growth in the tibia of mice placed on regular chow or LMPTP inhibitor formulated chow. With this model, we found inhibition of LMPTP reduced the tumor growth in bone. Altogether, we showed loss of LMPTP impaired the first and last steps of cancer metastasis.

However, it is worth noting \ we were unable to model other metastatic steps in between the initial invasion and the final colonization of bone. For example, we were unable to model prostate cancer cell migration through a monolayer of endothelial cells. This experiment would have allowed us to study the process of entering and exiting the blood vessels known as intravasation and extravasation, respectively[14]. To address this issue, we are currently working on developing an intracardiac injection mouse model. Using this model, Myc-CaP cells expressing luciferase (Luc-Myc-CaP cells) will be injected into the left ventricle of SCID mice to allow for the prostate cancer cells to enter the blood stream, travel around the body, and lodge itself into various organs. This model does not typically favor bone growth, but it can be used to observe extravasation out of the blood vessel and secondary tumor colonization, both of which are currently lacking from our project. Another metastatic component that is not documented by our study is the changes in the tumor microenvironment allowing for colonization and growth in the bone. Cancer cells typically send signals to neighboring fibroblasts and macrophages to prime the environment for optimal cancer cell survival[15]. Our tumorigenesis and intraosseous models address the ability of LMPTP to promote colonization of a new site, but we currently lack the understanding of whether LMPTP plays a role in altering the tumor microenvironment. We hope to address these

limitations in the future to further validate LMPTP as a relevant and promising metastatic prostate cancer therapeutic candidate.

In addition to establishing a growth and metastasis phenotype, we also hoped to uncover the molecular mechanism through which LMPTP promotes prostate cancer progression. Our phosphoproteomic results suggested that there was a difference in phosphorylation levels of molecules within the eIF2 signaling pathway between the WT and LMPTP KO cell lines. This eIF2 pathway is typically activated as a response to stressors in the cell including viral infection, amino acid starvation, and unfolded proteins[16]. Central to this integrated stress response (ISR) is the phosphorylation of eIF2 at Ser51 which then blocks the global translation of most proteins in favor for the translation of the activating transcription factor 4 (ATF4)[16]. ATF4 promotes the transcription of other genes that can reduce the current stress or in the worst-case scenario, induce apoptosis in the cell[16,17]. Although there was a significant difference in the phosphorylation of several affected molecules in the eIF2 pathway between WT and LMPTP KO prostate cancer cells, it was unclear which one was more activated based on the phosphoproteomic data alone. We hope to identify key interactors or substrates of LMPTP linked to eIF2 signaling. To pursue this further, we are currently using various types of stressors associated with the four kinases known to phosphorylate eiF2 at Ser51—the PKR-like ER kinase (PERK), protein kinase double-stranded RNA-dependent (PKR), general control non-derepressible-2 (GCN2), and heme-regulated inhibitor (HRI)[18]. This is being done in hopes of identifying how LMPTP is involved with eIF2 signaling. More specifically, we hope to understand whether this involvement is upstream or downstream eIF2 phosphorylation.

Our preliminary data showed that under a common stressor, such as serum starvation[18], LMPTP KO prostate cancer cells tend to undergo more eIF2 phosphorylation at Ser51. Serum starvation has been shown to increase the production of reactive oxygen species (ROS) in prostate cancer cells, and the presence of ROS increases oxidative stress[19]. Our data suggests that, in response to serum starvation and oxidative stress, LMPTP KO prostate cancer activate the eIF2 signaling pathway more would result in alleviation of stress or induction of cell death[16,17]. At the same time, our metabolomic data and bioluminescent glutathione (GSH) detection assay showed a striking reduction of GSH levels in the LMPTP KO prostate cancer cells compared to the WT. Glutathione is a known endogenous antioxidant that reduces the level of ROS found in cells[20]. Cells that undergo a lot of proliferation, such as cancer cells, tend to generate high levels of ROS[20]. Because LMPTP KO cells are deficient in GSH, there might be an accumulation of ROS that increases oxidative stress in LMPTP KO cells, which is further exacerbated when these cells are stripped of serum. The build up of stress and increase in eIF2 signaling could push the LMPTP KO prostate cancer cells towards cell death instead of alleviating the stressor. We are currently looking at ROS detection in cells and apoptosis assays to assess this model further.

Interestingly, the synergistic effect observed on prostate cancer cell growth due to loss of LMPTP combined with either of the two common prostate cancer drugs, Docetaxel and Cabaxitaxel, is consistent with our mechanistic model. Both Docetaxel and Cabazitaxel have been reported to either induce oxidative stress or generate ROS[21,22]. As such, LMPTP KO cells might be less equipped to deal with the oxidative stress induced by the two cancer drugs resulting in an even greater inhibition of growth

and activation of apoptosis. We are currently using flow cytometry to explore the effects of Docetaxel and Cabazitaxel on apoptosis and cell death in hopes of better understanding the potential combinatorial effect of LMPTP inhibition with either drug.

In this paper, we have established the oncogenic role of LMPTP in prostate cancer progression, proposed a mechanistic model to explain how LMPTP promotes prostate cancer, and established a synergistic effect between targeting LMPTP and current prostate cancer therapeutics. Altogether, we hope to introduce LMPTP inhibitors as a potential therapeutic drug for prostate cancer patients.

REFERENCES

1. Leslie, S. W., Soon-Sutton, T. L., Sajjad, H., & Siref, L. E. (2021). Prostate Cancer. In StatPearls. StatPearls Publishing.

2. Hanahan, D., & Weinberg, R. A. (2011). Hallmarks of cancer: the next generation. Cell, 144(5), 646–674. https://doi.org/10.1016/j.cell.2011.02.013

3. Sever, R., & Brugge, J. S. (2015). Signal transduction in cancer. Cold Spring Harbor perspectives in medicine, 5(4), a006098. https://doi.org/10.1101/cshperspect.a006098

4. Ardito, F., Giuliani, M., Perrone, D., Troiano, G., & Lo Muzio, L. (2017). The crucial role of protein phosphorylation in cell signaling and its use as targeted therapy (Review). International journal of molecular medicine, 40(2), 271–280. https://doi.org/10.3892/ijmm.2017.3036

5. Kannaiyan, R., & Mahadevan, D. (2018). A comprehensive review of protein kinase inhibitors for cancer therapy. Expert review of anticancer therapy, 18(12), 1249–1270. https://doi.org/10.1080/14737140.2018.1527688

6. Meeusen, B., & Janssens, V. (2018). Tumor suppressive protein phosphatases in human cancer: Emerging targets for therapeutic intervention and tumor stratification. The international journal of biochemistry & cell biology, 96, 98–134. https://doi.org/10.1016/j.biocel.2017.10.002

7. Das, S. K., Menezes, M. E., Bhatia, S., Wang, X. Y., Emdad, L., Sarkar, D., & Fisher, P. B. (2015). Gene Therapies for Cancer: Strategies, Challenges and Successes. *Journal of cellular physiology*, *230*(2), 259–271. https://doi.org/10.1002/jcp.24791

8. Frankson, R., Yu, Z. H., Bai, Y., Li, Q., Zhang, R. Y., & Zhang, Z. Y. (2017). Therapeutic Targeting of Oncogenic Tyrosine Phosphatases. Cancer research, 77(21), 5701–5705. https://doi.org/10.1158/0008-5472.CAN-17-1510

9. Caselli, A., Paoli, P., Santi, A., Mugnaioni, C., Toti, A., Camici, G., & Cirri, P. (2016). Low molecular weight protein tyrosine phosphatase: Multifaceted functions of an evolutionarily conserved enzyme. Biochimica et biophysica acta, 1864(10), 1339–1355. https://doi.org/10.1016/j.bbapap.2016.07.001

10. Ohtaka, M., Miyoshi, Y., Kawahara, T., Ohtake, S., Yasui, M., Uemura, K., Yoneyama, S., Hattori, Y., Teranishi, J. I., Yokomizo, Y., Uemura, H., Miyamoto, H., & Yao, M. (2017). Low-molecular-weight protein tyrosine phosphatase expression as a prognostic factor for men with metastatic hormone-naïve prostate cancer. Urologic oncology, 35(10), 607.e9–607.e14. https://doi.org/10.1016/j.urolonc.2017.05.019

11. Stanford, S. M., Aleshin, A. E., Zhang, V., Ardecky, R. J., Hedrick, M. P., Zou, J., Ganji, S. R., Bliss, M. R., Yamamoto, F., Bobkov, A. A., Kiselar, J., Liu, Y., Cadwell, G. W., Khare, S., Yu, J., Barquilla, A., Chung, T.D.Y., Mustelin, T., Schenk, S., Bankston, L. A., Liddington, R. C., Pinkerton, A. B., & Bottini, N. (2017). Diabetes reversal by inhibition of the low-molecular-weight tyrosine phosphatase. Nature chemical biology, 13(6), 624–632. https://doi.org/10.1038/nchembio.2344

12. Chandrashekar, D. S., Bashel, B., Balasubramanya, S., Creighton, C. J., Ponce-Rodriguez, I., Chakravarthi, B., & Varambally, S. (2017). UALCAN: A Portal for Facilitating Tumor Subgroup Gene Expression and Survival Analyses. Neoplasia (New York, N.Y.), 19(8), 649–658. https://doi.org/10.1016/j.neo.2017.05.002

13. Borowicz, S., Van Scoyk, M., Avasarala, S., Karuppusamy Rathinam, M. K., Tauler, J., Bikkavilli, R. K., & Winn, R. A. (2014). The soft agar colony formation assay. Journal of visualized experiments : JoVE, (92), e51998. https://doi.org/10.3791/51998

14. Welch, D. R., & Hurst, D. R. (2019). Defining the Hallmarks of Metastasis. Cancer research, 79(12), 3011–3027. https://doi.org/10.1158/0008-5472.CAN-19-0458

15. Sistigu, A., Musella, M., Galassi, C., Vitale, I., & De Maria, R. (2020). Tuning Cancer Fate: Tumor Microenvironment's Role in Cancer Stem Cell Quiescence and Reawakening. Frontiers in immunology, 11, 2166. https://doi.org/10.3389/fimmu.2020.02166

16. Pakos-Zebrucka, K., Koryga, I., Mnich, K., Ljujic, M., Samali, A., & Gorman, A. M. (2016). The integrated stress response. EMBO reports, 17(10), 1374–1395. https://doi.org/10.15252/embr.201642195

17. Hu, H., Tian, M., Ding, C., & Yu, S. (2019). The C/EBP Homologous Protein (CHOP) Transcription Factor Functions in Endoplasmic Reticulum Stress-Induced Apoptosis and Microbial Infection. Frontiers in immunology, 9, 3083. https://doi.org/10.3389/fimmu.2018.03083

18. Taniuchi, S., Miyake, M., Tsugawa, K., Oyadomari, M., & Oyadomari, S. (2016). Integrated stress response of vertebrates is regulated by four eIF2α kinases. Scientific reports, 6, 32886. https://doi.org/10.1038/srep32886

19. White, E. Z., Pennant, N. M., Carter, J. R., Hawsawi, O., Odero-Marah, V., & Hinton, C. V. (2020). Serum deprivation initiates adaptation and survival to oxidative stress in prostate cancer cells. Scientific reports, 10(1), 12505. https://doi.org/10.1038/s41598-020-68668-x

20. Bansal, A., & Simon, M. C. (2018). Glutathione metabolism in cancer progression and treatment resistance. The Journal of cell biology, 217(7), 2291–2298. https://doi.org/10.1083/jcb.201804161

21. Hung, C. H., Chan, S. H., Chu, P. M., & Tsai, K. L. (2015). Docetaxel Facilitates Endothelial Dysfunction through Oxidative Stress via Modulation of Protein Kinase C Beta: The Protective Effects of Sotrastaurin. Toxicological sciences : an official journal of the Society of Toxicology, 145(1), 59–67. https://doi.org/10.1093/toxsci/kfv017

22. Kosaka, T., Hongo, H., Miyazaki, Y., Nishimoto, K., Miyajima, A., & Oya, M. (2017). Reactive oxygen species induction by cabazitaxel through inhibiting Sestrin-3 in castration resistant prostate cancer. Oncotarget, 8(50), 87675–87683. https://doi.org/10.18632/oncotarget.21147